Trilinear Gauge Boson Couplings in the MSSM

E. N. Argyres [a*], **A. B. Lahanas** [b†], **C. G. Papadopoulos** [c,d**]
and   **V. C. Spanos** [c‡]

[a] NRCPS, 'Democritos', Aghia Paraskevi, GR – 15310 Athens, Greece
[b] University of Athens, Physics Department, Nuclear and Particle Physics Section,
GR – 15771 Athens, Greece
[c] University of Durham, Physics Department, Science Laboratories,
South Road, Durham DH1 3LE, England
[d] CERN, Theory Division, CH-1211, Geneva 23, Switzerland

Abstract

We study the C and P even $WW\gamma$ and WWZ trilinear gauge boson vertices (TGV's), in the context of the MSSM assuming that the external W's are on their mass shell. We find that for energies $\sqrt{s} \equiv \sqrt{q^2} \leq 200\ GeV$ squark and slepton contributions to the aforementioned couplings are two orders of magnitude smaller than those of the Standard Model (SM). In the same energy range the bulk of the supersymmetric Higgs corrections to the TGV's is due to the lightest neutral Higgs, h_0, whose contribution is like that of a Standard Model Higgs of the same mass. The contributions of the Neutralinos and Charginos are sensitive to the input value for the soft gaugino mass $M_{1/2}$, being more pronounced for values $M_{1/2} < 100\ GeV$. In this case and in the unphysical region, $0 < \sqrt{s} < 2M_W$, their contributions are substantially enhanced resulting in large corrections to the static quantities of the W boson. However, such an enhancement is not observed in the physical region. In general for $2M_W < \sqrt{s} < 200\ GeV$ the MSSM predictions differ from those of the SM but they are of the same order of magnitude. To be detectable deviations from the SM require sensitivities reaching the per mille level and hence unlikely to be observed at LEP200. For higher energies SM and MSSM predictions exhibit a fast fall off behaviour, in accord with unitarity requirements, getting smaller,in most cases, by almost an order of magnitude already at energies $\sqrt{s} \approx 0.5\ TeV$.

E-mail: *argyres@cyclades.nrcps.ariadne-t.gr,   †alahanas@atlas.uoa.ariadne-t.gr,
**papadopo@alice.nrcps.ariadne-t.gr, ‡V.C.Spanos@durham.ac.uk.

1. Introduction

The Standard Model (SM) has been remarkably successful in describing particle interactions at energies around $\sim 100\,GeV$. Precise measurements at LEP provided accurate tests of the standard theory of electroweak interactions [1, 2], but we are still lacking a direct experimental confirmation of the non-abelian structure of the standard theory. The $WW\gamma$, WWZ and $ZZ\gamma$ couplings are uniquely determined within the context of the SM and such couplings will be probed in the near future with high accuracy. The study of the trilinear gauge bosons vertices (TGV's) in the $e^+e^- \rightarrow W^+W^-$ process is the primary motivation for the upgrading of LEP200 [3] and the potential for measuring these has been discussed in detail [3, 4, 5]. So far there are no stringent experimental bounds on these couplings [6] and the efforts of the various experimental groups towards this direction are still continuing. Precise measurements of these vertices are of vital importance not only for the SM itself but also for probing new physics which may be revealed at scales larger than the Fermi scale.

The gauge boson vertex has been the subject of an intense theoretical study during the last years. In particular the WWV vertex ($V = \gamma$ or Z) has been analysed in detail within the framework of the standard theory, as well as extensions of it, and its phenomenology has been discussed. The lagrangian density describing the WWV interaction is given by [7, 8]

$$\mathcal{L}^{WWV} = -ig_{WWV}[(W^\dagger_{\mu\nu}W^\mu V^\nu - h.c.) + \kappa_V W^\dagger_\mu W_\nu F^{\mu\nu} + \frac{\lambda_V}{M_W^2}W^\dagger_{\lambda\mu}W^\mu_\nu V^{\nu\lambda} + ...]. \quad (1)$$

In this $g_{WWV} = e$ for $V = \gamma$ and $g_{WWV} = e \cot\theta_W$ for $V = Z$. The ellipsis stand for P or C odd terms and higher dimensional operators. In Eq. (1) the scalar components for all gauge bosons involved have been omitted, that is $\partial \cdot W = \partial \cdot V = 0$, since essentially they couple to massless fermions [1]. At the tree level κ_V and λ_V have the values $\kappa_V = 1$, $\lambda_V = 0$. However radiative corrections modify these, the order of magnitude of these corrections being $\mathcal{O}(\frac{\alpha}{\pi}) \sim 10^{-3}$. Sensitivity limits of this order of magnitude will not be reached at LEP200 but can be achieved in future colliders where the TGV's can be studied in detail and yield valuable information not only for the self consistency of the SM but also for probing underlying new physics. Any new dynamics whose onset lies in the TeV range modifies κ_V, λ_V and deviations from the SM predictions are expected.

Supersymmetry (SUSY) is an extension of the SM which is theoretically motivated but without any experimental confirmation [9]. The only experimental hint for its existence derives from the fact that the gauge couplings unify at energies $\sim 10^{16}\,GeV$, if we adopt a supersymmetric extension of the SM in which SUSY is broken at energies $M_{SUSY} \sim \mathcal{O}(1)\,TeV$ [10] . Supersymmetric particles with such large masses can be produced in the laboratory provided we have very high energies and luminocities. However, their existence affects κ_V and λ_V, even at energies lower than the SUSY production threshold making them deviate from the SM predictions. Therefore the study of these

---

[1]For on shell W's we have $(\Box + m_W^2)W_\mu = 0$ and certainly $\partial \cdot W = 0$, while for the photon $\partial \cdot A$ vanishes on account of current conservation.

quantities may furnish us with a good laboratory to look for signals of supersymmetry at energies below the SUSY production threshold. In any case such studies serve as a complementary test, along with other efforts, towards searching for signals of new physics and supersymmetry is among the prominent candidates.

In the SM κ_V and λ_V as functions of the momentum q^2 carried by the V boson ($V = \gamma, Z$), for on shell W's, have been studied in detail [11], but a similar analysis has not been carried out within the context of the MSSM. Only the quantities $\kappa_\gamma(q^2 = 0)$, $\lambda_\gamma(q^2 = 0)$ have been considered [12], which are actually related to the static magnetic dipole (μ_W) and electric quadrupole (Q_W) moments of the W boson. To be of relevance for future collider experiments the form factors $\kappa_{\gamma,Z}$, $\lambda_{\gamma,Z}$ should be evaluated in the region $q^2 > 4M_W^2$. The behavior of $\kappa_{\gamma,Z}$, $\lambda_{\gamma,Z}$ in this physical region may be different from that at $q^2 = 0$, especially when the energy gets closer to M_{SUSY} and supersymmetric particles may yield sizeable effects due to the fact that we are approaching their thresholds. In those cases an enhancement of their corresponding contributions is expected, unlike SM contributions which are suppressed in this high energy regime.

In this work we undertake this problem and study the C and P even $WW\gamma$, WWZ vertices in the context of the MSSM, with radiative electroweak symmetry breaking, when the external W bosons are on their mass shell. Such studies are important in view of forthcoming experiments at LEP200 and other future collider experiments which will probe the structure of the gauge boson couplings and test with high accuracy the predictions of the SM. If deviations from the SM predictions are observed these experiments will signal the presence of new underlying dynamics at scales larger than the Fermi scale.

1. The SM contribution to $\Delta k_V(Q^2)$, $\Delta Q_V(Q^2)$

Although the SM contributions to the TGV's have already been calculated in the literature [11], for reasons of completeness we shall briefly discuss them in this section paying special attention to the contributions of fermions and gauge bosons.

In momentum space the most general WWV vertex ($V = \gamma$ or Z) with the two W's on shell and keeping only the transvers degrees of freedom for the γ or Z can be writen as [7]

$$
\begin{aligned}
\Gamma^V_{\mu\alpha\beta} = & -ig_{WWV}\left\{ f_V[2g_{\alpha\beta}\Delta_\mu + 4(g_{\alpha\mu}Q_\beta - g_{\beta\mu}Q_\alpha)] \right. \\
& \left. +2\,\Delta k_V\,(g_{\alpha\mu}Q_\beta - g_{\beta\mu}Q_\alpha) + 4\,\frac{\Delta Q_V}{M_W^2}\,\Delta_\mu(Q_\alpha Q_\beta - \frac{Q^2}{2}g_{\alpha\beta})\right\} + ...
\end{aligned}
\tag{2}
$$

where $\Delta k_V \equiv \kappa_V + \lambda_V - 1$, $\Delta Q_V \equiv -2\,\lambda_V$. The kinematics of the vertex is shown in Fig. 1 .

The ordinary matter fermion contributions at $Q^2 = 0$ have been studied elsewhere [13, 14]. However in those works there is an important sign error which affects substantially the results given in those references [12]. This has also been pointed out independently in ref. [15] . The consequences of this for the static quantities of the

W boson μ_W, Q_W has been discussed in detail in ref. [12]. The fermion contributions to $\Delta k_\gamma(Q^2 = 0)$ are large and negative partially cancelling contributions of the gauge bosons and standard model Higgs which are positive.

At $Q^2 \neq 0$ and in units of $g^2/16\pi^2$ the fermion contributions of the graph shown in Fig. 1, when the internal lines are $(P_1, P_2, P_3) = (f, f, f')$, are given by,

$$
\begin{aligned}
\Delta k_V &= -c_V T_3^f C_g \int_0^1 dt \int_0^1 d\alpha \{ g_L^f [t^4 + t^3(-1 + R_{f'} - R_f) + t^2(R_f - R_{f'}) \\
&\quad + \frac{4Q^2}{M_W^2} t^3(3t-2)\alpha(1-\alpha)] + g_R^f [\, R_f\, t^2] \} \frac{1}{L_f^2}
\end{aligned}
\tag{3}
$$

$$
\Delta Q_V = -c_V T_3^f C_g\, g_L^f \int_0^1 dt \int_0^1 d\alpha \frac{8t^3(1-t)(1-\alpha)\alpha}{L_f^2}
\tag{4}
$$

where $c_\gamma = 1$, $c_Z = R$ with $R \equiv M_Z^2/M_W^2$. In Eqs. (3) and (4)

$$
L_f^2 \equiv t^2(1 - \frac{4Q^2}{M_W^2}\alpha(1-\alpha)) + t(R_f - R_{f'} - 1) + R_{f'} + i\epsilon \quad ,
$$

and C_g is the color factor (1 for leptons, 3 for quarks). Throughout this paper $R_i \equiv \frac{m_i^2}{M_W^2}$ where the index i refers to the relevant particle in each case. The couplings $g_{L,R}^f$ appearing in Eqs. (3) and (4) are $g_L^f = g_R^f = Q_{em}^f$ for $V = \gamma$, and $g_L^f = Q_{wL}^f, g_R^f = Q_{wR}^f$ for $V = Z$. Q_{em}^f are the electromagnetic charges, and $Q_{wL,R}^f$ are the weak charges for left/right handed fermions defined by the relation $Q_w^f \equiv T_3^f - Q_{em}^f \sin^2\theta_W$. T_3^f is the weak isospin of the fermion f, ie. $T_3^f = -1/2$ for the left handed charged leptons etc.

Regarding the contributions of the gauge bosons to Δk_V, ΔQ_V, $(Q^2 \neq 0)$, one faces the problem of gauge dependence. This is reflected in the loss of the crucial properties of infrared finiteness and perturbative unitarity. Analytic calculations of Δk_V, ΔQ_V were carried out in ref. [11] in the 't Hooft – Feynman gauge. In that reference it was shown that Δk_V has bad high energy behaviour, growing logarithmically as the energy increases, violating therefore unitarity constraints. At the same time Δk_V exhibits an infrared (IR) singularity the only one surviving among several others that cancel each other.

The problem of gauge dependence is simply related to the fact that in general n-point functions (propagators, vertices, etc) are not gauge invariant objects; only the S-matix elements have this property, being physically measurable quantities. Nevertheless there are several ways to extract the physically relevant information from their calculation. The most trivial example in our case, is to take the limit $Q^2 \to 0$, which defines the static properties of W boson. Less trivial is to consider special combinations of Δk_γ and Δk_Z which are directly measurable in the experiment. This is for instance the case of $e_L^+ e_R^- \to W^+ W^-$ reaction, where the combination $\Delta k_\gamma - 4Q^2/(4Q^2 - m_Z^2)\Delta k_Z$ can be measured. As is rather evident this combination is free of IR and gauge-dependence problems, as can be easily verified from the calculation of Δk_V [11].

Of course, the gauge-dependence cancels out when the full one-loop matrix element for a specific process, for instance $e^+e^- \rightarrow W^+W^-$, is performed. This means that the gauge-dependence of the three-point functions is eliminated from the corresponding contributions in the four-point functions. Therefore one can project out from the four-point functions the relevant tensor structures multiplying Δk_V and ΔQ_V and after collecting all possible contributions to the specific process a gauge invariant and physically relevant result would be obtained. Nevertheless this procedure would require the knowledge of the full one-loop contributions for each specific process. On the other hand one can proceed in this direction by employing special field theory methods such as the Pinch Technique (PT) in order to define gauge-invariant and process-independent quantities. The PT has been introduced by Cornwall [16] and has since been employed in various physical problems (see ref. [16] − [19]). The main feature of the PT algorithm, is that it enables us to define gauge-parameter independent self energies and vertices which satisfy QED-like Ward identities. More recent studies have explicitly demonstrated the universality of the PT-algorithm for gauge boson two point functions [19]. Another approach, through which gauge-parameter[2] and process independent quantities can also be obtained, is the Background Field Method (BFM) [20]. In principle, BFM provides a complementary and natural way to explain why the PT rules yield vertex functions that have the desirable properties and satisfy simple Ward identities.

More specifically in our case PT provides us with an algorithm to isolate from box graphs pieces that have a vertex like structure and allot them to the usual vertex graphs. The details of this proceedure and the way one extracts the relevant pinch parts $\Delta \hat{k}_{\gamma,Z}$ can be traced in ref. [17]. Once the pinch contribution are taken into account the gauge boson contributions to TGV's become gauge independent approaching zero values as Q^2 increases, as demanded by unitarity, being also free of infrared singularities.

Furthermore, by an explicit calculation, it can be shown that the pinch parts do not contribute when the incoming electron carries right handed chirality, as expected. In fact in that case the particular combination entering the amplitude for the process $e_L^+ e_R^- \rightarrow W^+W^-$ has vanishing pinch part and hence in such a process only the genuine vertex parts contribute[11].

In the sequel and in order to keep our discussion independent of the specific process as much as possible we shall consider the SM contributions with the pinch parts properly incorporated into the usual vertex contributions. As yet, there is no systematic study of how well the PT approximates the coefficient of the relevant tensor structures of the full one-loop result in specific processes. Nevertheless, we shall use it as a basis for comparison of the supersymmetric contributions which are well behaved and not plagued by gauge dependent or infrared pathologies.

---

[2]With respect to gauge transformations of the background field.

4

2. The MSSM contribution to $\Delta k_V(Q^2)$, $\Delta Q_V(Q^2)$

The MSSM is described by a Lagrangian [9]

$$\mathcal{L} = \mathcal{L}_{SUSY} + \mathcal{L}_{soft} \tag{5}$$

where $\mathcal{L}_{SUSY}$ is its supersymmetric part and $\mathcal{L}_{soft}$ the SUSY breaking part. A convenient set of parameters to describe low energy physics is given by

$$m_0 \quad , \quad A_0 \quad , \quad M_{1/2} \quad , \quad \tan\beta(M_Z) \quad , \quad m_t(M_Z), \tag{6}$$

where $m_0, A_0, M_{1/2}$ are the soft SUSY breaking parameters, $m_t(M_Z)$ is the value of the "runing" top quark mass at the Z - boson pole mass M_Z, and $\tan\beta(M_Z)$ the ratio of the v.e.v's of the Higgses H_2, H_1. Complete expressions for the RGE's of all parameters involved can be found in the literature and will not be repeated here [9].

At $Q^2 = 0$ the MSSM contributions to Δk_γ, ΔQ_γ have been studied elsewhere and their dependences on the soft breaking parameters A, m_0, $M_{1/2}$, $\tan\beta$ and top quark mass m_t have been investigated [12]. In summary the conclusions reached in that paper are as follows :

i) Squarks and Sleptons have negligible effect on the dipole and quadrupole moments as compared to contributions of other sectors.

ii) The bulk of the MSSM Higgs contributions to Δk_γ, ΔQ_γ is due to the lightest CP - even neutral h_0, whose one loop corrected mass does not exceed $\approx 140 GeV$.

iii) The Neutralinos and Charginos under certain conditions may be the dominant source of substantial deviations from the SM predictions. This happens for values of the soft gaugino mass $M_{1/2} \ll A_0, m_0$. In some extreme cases their contributions can even saturate the LEP200 sensitivity limits.

The question of whether sizeable deviations from the SM predictions can show up at nonzero values of Q^2, accessible at LEP200 or other future colliders, is our principal motivation to study the behaviour of aforementioned quantities in the $Q^2 \neq 0$ region.

In the MSSM gauge boson and ordinary fermion contributions are like those of the SM and will be treated in the way desrcibed in the previous section. The additional contributions from $\tilde{q}, \tilde{l}$ (squarks, sleptons), $\tilde{Z}, \tilde{C}$ (neutralinos, charginos) as well as the supersymmetric Higgs contributions to Δk_V, ΔQ_V can be deduced from the triangle graph shown in Figure 1 where $P_{1,2,3}$ are the appropriate internal lines. We will not consider graphs that yield vanishing contributions to both Δk_V and ΔQ_V.

In the following we shall consider the contributions of each sector separately.

Squarks–Sleptons ($\tilde{q}$, $\tilde{l}$)

We first consider the contributions of the sfermion sector of the theory which can be read from the diagram of Figure 1 with the assignment $P_1 = P_2 = \tilde{f}, P_3 = \tilde{f}'$ to the internal lines. $\tilde{f}$ and $\tilde{f}'$ denote sfermions. Unlike matter fermions this graph involves mixing matrices due to the fact that left $\tilde{f}_L$ and right $\tilde{f}_L^c$ handed sfermions mix when

electroweak symmetry breaks down. Such mixings are substantial in the stops, due to the heaviness of the top quark, resulting in large mass splittings of the corresponding mass eigenstates $\tilde{t}_{1,2}$.

In units of $g^2/16\pi^2$ the sfermion contributions are given by:

$$
\begin{aligned}
\Delta k_V &= -2C_g c_V T_3^f \sum_{i,j,k=1}^{2} (A_{ij}^{V,\tilde{f}} K_{i1}^{\tilde{f}} K_{j1}^{\tilde{f}})(K_{k1}^{\tilde{f}'} K_{k1}^{\tilde{f}'}) \\
&\quad \times \int_0^1 dt \int_0^1 d\alpha \frac{t^2(1-t)[2t-1+R_{\tilde{f}_i}\alpha + R_{\tilde{f}_j}(1-\alpha) - R_{\tilde{f}_k'}]}{L_{\tilde{f}\tilde{f}'}^2}
\end{aligned}
\tag{7}
$$

$$
\begin{aligned}
\Delta Q_V &= 8C_g c_V T_3^f \sum_{i,j,k=1}^{2} (A_{ij}^{V,\tilde{f}} K_{i1}^{\tilde{f}} K_{j1}^{\tilde{f}})(K_{k1}^{\tilde{f}'} K_{k1}^{\tilde{f}'}) \\
&\quad \times \int_0^1 dt \int_0^1 d\alpha \frac{t^3(1-t)\alpha(1-\alpha)}{L_{\tilde{f}\tilde{f}'}^2}
\end{aligned}
\tag{8}
$$

where

$$
L_{\tilde{f},\tilde{f}'}^2 \equiv t^2 + (R_{\tilde{f}_i}\alpha + R_{\tilde{f}_j}(1-\alpha) - 1)t + R_{\tilde{f}_k'}(1-t) - \frac{4Q^2}{M_W^2}t^2\alpha(1-\alpha) + i\epsilon.
$$

In the expressions above $A_{ij}^{V,\tilde{f}}$ are given by, $A_{ij}^{Z,\tilde{f}} = Q_W^{\tilde{f}}\delta_{ij} - T_3^{\tilde{f}} K_{i2}^{\tilde{f}} K_{j2}^{\tilde{f}}$, $A_{ij}^{\gamma,\tilde{f}} = Q_{em}^{\tilde{f}}\delta_{ij}$ where $Q_W^{\tilde{f}}$ and $Q_W^{\tilde{f}} \equiv T_3^{\tilde{f}} - Q_{em}^{\tilde{f}}\sin^2\theta_W$ are the electromagnetic and weak charges of the sfermion $\tilde{f}$ respectively. The remaining factors c_γ, c_Z , and C_g were defined in the previous section. $\tilde{f}_{1,2}$ and $\tilde{f}'_{1,2}$ denote the mass eigenstates while $\mathbf{K}^{\tilde{f},\tilde{f}'}$ diagonalize the corresponding mass matrices (for notation see ref.[12]). In the stop sector for instance, the diagonalizing matrix is defined as $\mathbf{K}^{\tilde{t}}\mathcal{M}_{\tilde{t}}^2\mathbf{K}^{\tilde{t}\mathbf{T}} = diagonal(m_{\tilde{t}_1}^2, m_{\tilde{t}_2}^2)$. In the absence of SUSY breaking effects $m_{\tilde{f},\tilde{f}'} = m_{f,f'}$ and $\mathbf{K}^{\tilde{f},\tilde{f}'}$ become the unit matrices. In that limit ΔQ_V given above cancels against the corresponding fermionic contribution of Eq. (4) as it should.

Neutralinos–Charginos ($\tilde{Z}$, $\tilde{C}$)

The neutralino and chargino sector is perhaps the most awkward sector to deal with due to mixings originating from the electroweak symmetry breaking effects. The two charginos $\tilde{C}_i$ (Dirac fermions) and the four neutralinos $\tilde{Z}_\alpha$ (Majorana fermions) are eigenstates of the mass matrices $\mathcal{M}_{\tilde{C}}$ and $\mathcal{M}_{\tilde{N}}$ whose explicit expressions can be found in ref. [12]. If the $\mathbf{U}$, $\mathbf{V}$ matrices diagonalize $\mathcal{M}_{\tilde{C}}$, i.e. $\mathbf{U}\mathcal{M}_{\tilde{C}}\mathbf{V}^\dagger = diagonal$, and $\mathbf{O}$ (real orthogonal) diagonalizes the real symmetric neutralino mass matrix $\mathcal{M}_{\tilde{N}}$, $\mathbf{O^T}\mathcal{M}_{\tilde{N}}\mathbf{O} = diagonal$, then their electromagnetic and weak currents are given by

$$
J_{em}^\mu = \sum_i \bar{\tilde{C}}_i \gamma^\mu \tilde{C}_i \quad , \quad J_+^\mu = \sum_{\alpha,i} \bar{\tilde{Z}}_\alpha \gamma^\mu (P_R C_{\alpha i}^R + P_L C_{\alpha i}^L)\tilde{C}_i
$$

$$
J_0^\mu = \sum_{i,j} \bar{\tilde{C}}_i \gamma^\mu (P_R A_{ij}^R + P_L A_{ij}^L)\tilde{C}_j + \frac{1}{2}\sum_{\alpha,\beta} \bar{\tilde{Z}}_\alpha \gamma^\mu (P_R B_{\alpha\beta}^R + P_L B_{\alpha\beta}^L)\tilde{Z}_\beta
$$

where

$$C_{\alpha i}^R = -\frac{1}{\sqrt{2}}O_{3\alpha}U_{i2}^* - O_{2\alpha}U_{i1}^* \ , \ \ C_{\alpha i}^L = +\frac{1}{\sqrt{2}}O_{4\alpha}V_{i2}^* - O_{2\alpha}V_{i1}^* \tag{9}$$

$$A_{ij}^h = [\cos^2\theta_W \delta_{ij} - \frac{1}{2}(V_{i2}V_{j2}^*\delta_{hL} + U_{i2}^*U_{j2}\delta_{hR})] \ , \ \ h = L, R \tag{10}$$

$$B_{\alpha\beta}^L = \frac{1}{2}(O_{3\alpha}O_{3\beta} - O_{4\alpha}O_{4\beta}) \ \ , \ \ B_{\alpha\beta}^R = -B_{\alpha\beta}^L \ . \tag{11}$$

$P_{R,L}$ are the right/left−handed projection operators $(1 \pm \gamma_5)/2$.

The contributions of this sector to Δk_γ, ΔQ_γ, which are given below, are calculated from the graph of Figure 1, with the following assignments to the internal lines $P_{1,2,3}$,

$\underline{(P_1, P_2, P_3) = (\tilde{C}, \tilde{C}, \tilde{Z})}$:

$$\Delta k_\gamma = -\sum_{i,\alpha} \int_0^1 dt \int_0^1 d\alpha \{F_{\alpha i}[t^4 + (R_\alpha - R_i - 1)t^3 + (2R_i - R_\alpha)t^2$$

$$+\frac{4Q^2}{M_W^2}t^3(3t-2)\alpha(1-\alpha)] + G_{\alpha i}\frac{m_i m_\alpha}{M_W^2}(4t^2 - 2t)\}\frac{1}{L_{\tilde{Z}}^2} \tag{12}$$

$$\Delta Q_\gamma = -8\sum_{i,\alpha} F_{\alpha i} \int_0^1 dt \int_0^1 d\alpha \frac{t^3(1-t)\alpha(1-\alpha)}{L_{\tilde{Z}}^2}, \tag{13}$$

where $\quad F_{\alpha i} = |C_{\alpha i}^R|^2 + |C_{\alpha i}^L|^2 \quad, \quad G_{\alpha i} = (C_{\alpha i}^L C_{\alpha i}^{R*} + h.c.)$, and

$$L_{\tilde{Z}}^2 = t^2 + (R_i - R_\alpha - 1)t + R_\alpha - \frac{4Q^2}{M_W^2}t^2\alpha(1-\alpha) + i\epsilon. \tag{14}$$

In the equations above the indices $\alpha = 1, 2, 3, 4$ and $i = 1, 2$ refer to neutralino and chargino states respectively. Note that we have not committed ourselves to a particular sign convention for the masses m_i, m_α appearing in the sum in the equation above for the Δk_γ. Chiral rotations that make these masses positive also affect the rotation matrices and should be taken into account.

For the couplings Δk_Z, ΔQ_Z we have the following contributions

i) $\quad \underline{(P_1, P_2, P_3) = (\tilde{C}, \tilde{C}, \tilde{Z})}$:

$$\Delta k_Z = -R \sum_{i,j,\alpha} \int_0^1 dt \int_0^1 d\alpha \{S_{ij\alpha}^L[t^2(1-t)(-t + R_i\alpha + R_j(1-\alpha) - R_\alpha)$$

$$+\frac{4Q^2}{M_W^2}t^3(3t-2)\alpha(1-\alpha)] + \frac{m_i m_j}{M_W^2}S_{ij\alpha}^R t^2$$

$$-\frac{m_i m_\alpha}{M_W^2}(T_{ij\alpha}^L + T_{ij\alpha}^R)[2t^2\alpha + t^2 - t]\}\frac{1}{L_{ij\alpha}^2} \tag{15}$$

$$\Delta Q_Z = -8R \sum_{i,j,\alpha} S_{ij\alpha}^L \int_0^1 dt \int_0^1 d\alpha \frac{t^3(1-t)\alpha(1-\alpha)}{L_{ij\alpha}^2} \tag{16}$$

7

where

$$S_{ij\alpha}^{L(R)} \equiv (C_{\alpha i}^{L*}C_{\alpha j}^{L}A_{ji}^{L(R)} + (L \rightleftharpoons R)) \quad , \quad T_{ij\alpha}^{L(R)} \equiv (C_{\alpha i}^{L*}C_{\alpha j}^{R}A_{ji}^{L(R)} + (L \rightleftharpoons R))$$

$$L_{ij\alpha}^{2} = \alpha t R_i + t(1-\alpha)R_j + R_\alpha(1-t) - t(1-t) - \frac{4Q^2}{M_W^2}t^2\alpha(1-\alpha) + i\epsilon$$

The indices i, j refer to charginos and α to neutralino mass eigenstates.

ii) $\underline{(P_1, P_2, P_3) = (\tilde{Z}, \tilde{Z}, \tilde{C})}$:

This is the same as the previous graph with $\{i, j, \alpha\}$ replaced by $\{\rho, \sigma, i\}$ and $S_{ij\rho}^{L(R)}, T_{ij\rho}^{L(R)}$, $L_{ij\alpha}^2$ replaced by the following expressions:

$$S_{\rho\sigma i}^{\prime L(R)} \equiv -(C_{\rho i}^{L*}C_{\sigma i}^{L}B_{\rho\sigma}^{L(R)} + (L \rightleftharpoons R)) \quad , \quad T_{\rho\sigma i}^{\prime L(R)} \equiv -(C_{\rho i}^{R*}C_{\sigma i}^{L}B_{\rho\sigma}^{L(R)} + (L \rightleftharpoons R))$$

$$L_{\rho\sigma i}^{\prime 2} = \alpha t R_\rho + t(1-\alpha)R_\sigma + R_i(1-t) - t(1-t) - \frac{4Q^2}{M_W^2}t^2\alpha(1-\alpha) + i\epsilon$$

In these σ, ρ refer to neutralinos and i to chargino mass eigenstates.

Higgses $(H_0, h_0, A, H_\pm)$

There are five physical Higgs bosons which survive electroweak symmetry breaking. Two of these, H_0 and h_0, are neutral and CP even, while a third A, is neutral and CP odd. The remaining Higgs bosons, $H_\pm$, are charged. At the tree level the lightest of these, namely h_0, is lighter than the Z gauge boson itself. However it is well known that radiative corrections, which are due to the heavy top, are quite large and may push its mass above M_Z. h_0 turns out to yield the largest contributions of all Higgses to the TGV's, since the remaining Higgses have large masses of the order of the SUSY breaking scale. At the tree level the masses of all Higgs bosons involved are given by the following expressions :

$$m_A^2 = -\frac{2B\mu}{\sin 2\beta} \quad , \quad m_{H_\pm}^2 = m_A^2 + M_W^2 \tag{17}$$

$$m_{H_0,h_0}^2 = \frac{1}{2}\{(m_A^2 + M_Z^2)^2 \pm \sqrt{(m_A^2 + M_Z^2)^2 - 4M_Z^2 m_A^2 cos^2(2\beta)}\} \tag{18}$$

The Higgs contributions can be expressed in terms of their masses and an angle θ, which relates the states $S_1 \equiv \cos\beta \, (Real \, H_1^0) + \sin\beta \, (Real \, H_2^0)$, $S_2 \equiv -\sin\beta \, (Real \, H_1^0) + \cos\beta \, (Real \, H_2^0)$ to the mass eigenstates h_0, H_0. The state S_1 is the SM Higgs boson, which however is not a mass eigenstate since it mixes with S_2. When $\sin^2\theta = 1$ such a mixing does not occur and h_0 becomes the standard model Higgs boson S_1.

The various contributions of the Higgs bosons to Δk_γ, ΔQ_γ, are given below. The assignment to the internal lines (P_1, P_2, P_3) in each case is explicitly shown:

i) $\quad \underline{(P_1, P_2, P_3) = (H_+, H_-, A)}$:

$$\Delta k_\gamma = D_2(R_A, R_{H_+}) \quad , \quad \Delta Q_\gamma = Q(R_A, R_{H_+}) \tag{19}$$

ii) $\quad \underline{(P_1, P_2, P_3) = (W_+, W_-, h_0) + (H_+, H_-, h_0)}$:

$$\Delta k_\gamma = \sin^2 \theta \, D_1(R_{h_0}) + \cos^2 \theta \, D_2(R_{h_0}, R_{H_+}) \tag{20}$$

$$\Delta Q_\gamma = \sin^2 \theta \, Q(R_{h_0}, 1) + \cos^2 \theta \, Q(R_{h_0}, R_{H_+}) \tag{21}$$

iii) $\quad \underline{(P_1, P_2, P_3) = (W_+, W_-, H_0) + (H_+, H_-, H_0)}$:

$$As \quad in \ ii) \quad with \quad R_{h_0} \to R_{H_0} \quad and \quad \sin^2 \theta \rightleftharpoons \cos^2 \theta \tag{22}$$

where $\sin^2 \theta = (M_A^2 + M_Z^2 \sin^2 2\beta - M_{h_0}^2)/(M_{H_0}^2 - M_{h_0}^2)$. The functions $D_{1,2}, Q$ appearing above are given by

$$D_1(r) \equiv \frac{1}{2} \int_0^1 dt \int_0^1 d\alpha \frac{2t^4 + (-2-r)t^3 + (4+r)\,t^2}{t^2 + r(1-t) - \frac{4Q^2}{M_W^2}t^2\alpha(1-\alpha) + i\epsilon} \tag{23}$$

$$D_2(r, R) \equiv \frac{1}{2} \int_0^1 dt \int_0^1 d\alpha \frac{2t^4 + (-3-r+R)t^3 + (1+r-R)t^2}{t^2 + (-1-r+R)t + r - \frac{4Q^2}{M_W^2}t^2\alpha(1-\alpha) + i\epsilon} \tag{24}$$

$$Q(r, R) \equiv 2 \int_0^1 dt \int_0^1 d\alpha \frac{t^3(1-t)\alpha(1-\alpha)}{t^2 + (-1-r+R)t + r - \frac{4Q^2}{M_W^2}t^2\alpha(1-\alpha) + i\epsilon} \tag{25}$$

For the Δk_Z, ΔQ_Z form factors we get the following contributions:

i) $\quad \underline{(P_1, P_2, P_3) = (W_+, W_-, h_0 + H_0)}$:

$$\Delta k_Z = \frac{1}{4}\{(\cos^2 \theta) \int_0^1 dt \int_0^1 d\alpha \, [(4 - 2R)t^4 + (R-2)(R_{H_0} + 2)t^3$$
$$+ (2R_{H_0} - RR_{H_0} + 8 - 2R)t^2]\frac{1}{L_{H_0}^2} + (\sin^2 \theta) \times (H_0 \to h_0)\} \tag{26}$$

$$\Delta Q_Z = (2-R)\{(\cos^2 \theta) \int_0^1 dt \int_0^1 d\alpha \frac{t^3(1-t)\alpha(1-\alpha)}{L_{H_0}^2}$$
$$+ (\sin^2 \theta) \times (H_0 \to h_0)\} \tag{27}$$

where $\quad L_{H_0}^2 \equiv t^2 + R_{H_0}(1-t) - \frac{4Q^2}{M_W^2}t^2\alpha(1-\alpha) + i\epsilon$.

ii) $\quad \underline{(P_1, P_2, P_3) = (H_+, H_-, A + H_0 + h_0)}$:

$$\Delta k_Z = (\frac{2-R}{2})\{D_2(R_A, R_{H_+}) + \sin^2 \theta \, D_2(R_{H_0}, R_{H_+}) + \cos^2 \theta \, D_2(R_{h_0}, R_{H_+})\} \tag{28}$$

$$\Delta Q_Z = (\frac{2-R}{2})\{Q(R_A, R_{H_+}) + \sin^2 \theta \, Q(R_{H_0}, R_{H_+}) + \cos^2 \theta \, Q(R_{h_0}, R_{H_+})\} \tag{29}$$

9

iii)　　$\underline{(P_1, P_2, P_3) = (H_0 + h_0, A, H_+) + (A, H_0 + h_0, H_+)}$:

$$\Delta k_Z = \frac{R}{2}\{(\sin^2\theta)\int_0^1 dt \int_0^1 d\alpha\, \frac{t^2(1-t)(1 + R_{H_+} - R_A\alpha - R_{H_0}(1-\alpha) - 2t)}{\tilde{L}^2_{H_0}}$$
$$+ (\cos^2\theta) \times (H_0 \to h_0)\} \qquad (30)$$

$$\Delta Q_Z = 2R\{(\sin^2\theta)\int_0^1 dt \int_0^1 d\alpha \frac{\alpha(1-\alpha)t^3(1-t)}{\tilde{L}^2_{H_0}} + (\cos^2\theta) \times (H_0 \to h_0)\} \qquad (31)$$

with　$\tilde{L}^2_{H_0} \equiv -t(1-t) + R_A\alpha t + R_{H_0}(1-\alpha)t + R_{H_+}(1-t) - \frac{4Q^2}{M_W^2}t^2\alpha(1-\alpha) + i\epsilon$,
and finally,

iv)　　$\underline{(P_1, P_2, P_3) = (Z, H_0 + h_0, W_+) + (H_0 + h_0, Z, W_+)}$:

$$\Delta k_Z = \frac{R}{2}\{(\cos^2\theta)\int_0^1 dt \int_0^1 d\alpha\, [-6\alpha t^2 + (t^3 - t^2)(2(t-1) + (R - R_{H_0})\alpha + R_{H_0})$$
$$+ 2(R-1)\alpha t^2]\frac{1}{\hat{L}^2_{H_0}} + (\sin^2\theta) \times (H_0 \to h_0)\} \qquad (32)$$

$$\Delta Q_Z = 2R\{(\cos^2\theta)\int_0^1 dt \int_0^1 d\alpha \frac{\alpha(1-\alpha)t^3(1-t)}{\hat{L}^2_{H_0}}\} + (\sin^2\theta) \times (H_0 \to h_0)\} \qquad (33)$$

with $\hat{L}^2_{H_0} \equiv (1-t)^2 + R\alpha t + R_{H_0}t(1-\alpha) - \frac{4Q^2}{M_W^2}t^2\alpha(1-\alpha) + i\epsilon$.

In most of the parameter space the Higgses $A, H_\pm$ and H_0 turn out to be rather heavy with masses of the order of the SUSY breaking scale; therefore all graphs in which at least one of these participates are small. At the same time $\sin^2\theta$ has a value very close to unity. Thus the dominant Higgs contribution arises solely from graphs in which a h_0 is exchanged. This is exactly what one gets in the SM with h_0 playing the role of the SM Higgs boson.

The form factors considered so far develop also imaginary (absortive) parts which show up as we cross the thresholds of internal particles in the loop. These can be calculated using the $i\epsilon$ prescription. Note also that the pinch parts discussed before have imaginary parts which should be taken into account as we do. The absortive parts contribute to physical processes too and therefore for a complete analysis their behaviour as a function of the energy should be studied. For lack of space in this paper we do not display analytic expressions for the imaginary parts. Their behaviour as a function of the variable Q^2 will be discussed in our conclusion part.

3. Numerical Analysis – Conclusions

Both dispersive and absortive parts of the trilinear $WW\gamma$, WWZ vertices can be cast in the form of single integrals of known functions of t and Q^2, which also depend on the physical masses of all particles involved. In fact wherever double $\int_0^1 dt \int_0^1 d\alpha$ integrations are encountered we first perform the $\int_0^1 d\alpha$ integrations explicitly and subsequently carry out the $\int_0^1 dt$ integrations numerically using special routines of the FORTRAN Library $IMSL$. The advantage of using this facility is that it leads to reliable results even in cases where the integrands exhibit fast growth at some points or have a rapid oscillatory behaviour. The inputs in these calculations are the variable Q^2 and the arbitrary parameters of the MSSM.

With the experimental inputs $M_Z = 91.188\, GeV$, $\sin^2\theta_W = .232$, $\alpha_{em}(M_Z) = 1/127.9$ and $\alpha_s(M_Z) = .115$ and with given values for the arbitrary parameters $\tan\beta(M_Z)$, $m_t(M_Z)$, A_0, m_0, $M_{1/2}$ we ran our numerical routines in order to know the mass spectrum and the relevant mixing parameters necessary for the evaluation of the form factors given in the previous sections. For the running top quark mass $m_t(M_Z)$ we took values in the whole range from $130\, GeV$ to $190\, GeV$, although small values of m_t are already ruled out in view of the CDF and $D0$ results [21]. The physical top quark masses emerging are slightly larger by about 3%

As for the soft SUSY breaking parameters $A_0, m_0, M_{1/2}$ we scan the three dimensional parameter space from $\simeq 100\, GeV$ to $1\, TeV$. This parameter space can be divided into three main regions i) $A_0 \simeq m_0 \simeq M_{1/2}$ (SUSY breaking terms comparable), ii) $A_0 \simeq m_0 \ll M_{1/2}$ (the gaugino mass is the dominant source of SUSY breaking) and iii) $M_{1/2} \ll A_0 \simeq m_0$ (A_0, m_0 dominate over $M_{1/2}$) . Case ii) covers the no-scale models for which the preferable values are $A_0 = m_0 = 0$, while case iii) covers the light gluino case.

Regarding the values scanned for the energy variable Q^2 we explored both the timelike and spacelike regions for values ranging from $\mid Q^2 \mid = 0$ to $\mid Q^2 \mid = 10^5 M_W^2$. For the timelike case, which is of relevance for future collider experiments, this corresponds to values of $\sqrt{s}$ ranging from $0\, GeV$ to about $600\, M_W$. Both in the spacelike and timelike energy region we have seen that as soon as $\sqrt{s}$ exceeds $\simeq$ few TeV the contributions of each sector separately becomes negligible, approaching zero as the energy increases in accord with unitarity requirements.

Sample results are presented in Table 1 for values of $(A_0, m_0, M_{1/2})$ equal to $(300, 300, 300)$, $(0, 0, 300)$ and $(300, 300, 80)\, GeV$ representative of the cases i),ii) and iii) discussed previously. The inputs for the remaining parameters are $tan\beta(M_Z) = 2$, $m_t(M_Z) = 170 GeV$. The value of $\sqrt{s}$ in these tables are respectively 190 and $500 GeV$, corresponding to the center of mass energies of LEP200 and NLC. [3] In the same table for comparison we give the SM predictions for Higgs masses equal to $50, 100$ and $300\, GeV$. With the inputs given above the typical SUSY breaking scale lies somewhere between $2M_W$ and $0.5\, TeV$. Although many sparticle thresholds exist in this region, as for instance the lightest of the sleptons and squarks as well as the lightest of the neutralinos and charginos,

---

[3]Throughout this paper whenever we refer to MSSM predictions we mean both sparticle and particle contributions, gauge boson and ordinary fermion contributions inclusive.

especially when $M_{1/2}$ is light, these thresholds do not result in any enhancement of the form factors $\Delta k_{\gamma,Z}$, $\Delta Q_{\gamma,Z}$. Increasing the value of the dominant SUSY breaking scale the supersymmetric contributions to these quantities become less important approaching zero values.

We now come to discuss separately the contributions of sparticles and supersymmetric Higgses. The sfermions yield the smaller contributions even in cases where due to large electroweak mixings some of the squarks, namely one of the stops, are relatively light. The supersymmetric Higgses yield contributions comparable to those of the SM, provided the latter involves a light Higgs with mass around $100\,GeV$. The bulk of the Higgs contributions is due to the lightest CP even neutral h_0. Thus SUSY Higgs contributions are like those of the SM with h_0 playing the role of the Standard Model Higgs boson. The neutralinos and charginos in some cases, depending on the given inputs, can accomodate light states. Their contributions in that case are not necessarily suppressed and are the principal source of deviations from the SM predictions. The contributions of this sector are sensitive to the input value for the soft gaugino mass $M_{1/2}$, being more important for values $M_{1/2} < 100\,GeV$. For such values of the soft gaugino mass and in the region, $0 < \sqrt{s} < 2M_W$ their contributions are enhanced, due to the development of an anomalous threshold, resulting to sizeable corrections to the magnetic dipole and electric quadrupole moments of the W boson [12]. However such an enhancement does not occur in the physical region and these contributions fall rapidly to zero as we depart from the unphysical region to values of energies above the two W production threshold.

The total contributions to the $\Delta k_{\gamma,Z}$, for some particular cases, both in the MSSM and SM are shown in Figure 2 for values of $\sqrt{s}$ ranging from $0\,GeV$ to $1\,TeV$. The region from 0 to $2M_W$ is unphysical since the external W's have been taken on their mass shell. At $s = 0$ the quantities Δk_γ, ΔQ_γ are linearly related to the magnetic moment and electric quadrupole moments of the W-boson. The MSSM predictions displayed in Figure 2 are for the particular choice $(A_0, m_0, M_{1/2}) = (300, 300, 80)$, the most interesting of the three cases discussed previously, since it includes light neutralino and chargino states. We only show the $\mu > 0$ case. The negative μ case leads to similar results. For lack of space we have only displayed the dispersive part. The absortive part turns out to have qualitatively a similar behaviour and we will not discuss them any further. All form factors tend to zero fairly soon with increasing energy reaching their asymptotic values at energies $\sqrt{s} \approx few\,TeV$ in agreement with unitarity constraints. The first peak observed in the unphysical region ($\sqrt{s} < 2M_W$) in the MSSM is due to the anomalous threshold of the Neutralino/Chargino sector discussed previously. In the physical region ($\sqrt{s} > 2M_W$) the first peak observed is associated with the $t\bar{t}$ production threshold while the second, around $700\,GeV$, is due to the threshold of the heavy neutralino states. We should point out that if it were not for the Neutralino/Chargino sector the MSSM and SM predictions would differ little. This sector is therefore the dominant source of deviations from the Standard Model predictions provided it accomodates light states.

The TGV's studied in this paper have been promoted to physical observables as being gauge independent satisfying at the same time the perturbative unitarity requirements, using the PT algorithm. The question of how to extract physical information on

these vertices from measurements of physical processes at e^+e^- and hadron colliders has been the subject of many phenomenological studies and has recently triggered numerous debates among physicists in working groups at LEP200 [22] and other workshops [D. Zeppenfeld in [5], [23]]. $WW\gamma$ and WWZ vertices are parts of the experimentally observed amplitudes of the $e^+e^- \rightarrow W^+W^-$ process whose SM radiative corrections have been studied elsewhere [24]. The accuracy of measuring the aforementioned vertices is improved with polarized beams. In this case, it is the particular combination $\Delta k_\gamma - 4Q^2/(4Q^2 - m_Z^2)\Delta k_Z$ which enters the amplitude for the reaction $e_L^+e_R^- \rightarrow W^+W^-$ [7, 25], and this is gauge independent and free of infrared singularities. Moreover it is independent of the PT algorithm, as we have already discused. Its behaviour as a function of the energy is displayed in Figure 3 for both MSSM and SM. The parameters are as in Figure 2. In the MSSM both $\mu > 0$ and $\mu < 0$ cases are shown. One notices that MSSM and SM predictions for this quantity are very close to one another apart from the peak which is due to the heavy neutralino threshold. Differences however are small, and to be detected requires high sensitivities.

In our analysis we have focused our attention on the TGV's considering all SUSY contributions to them. For a complete one loop analysis of the $e^+e^- \rightarrow W^+W^-$ process the SUSY box contributions should be taken into account. There is no a priori reason why these should be small. However these graphs involve exchanges of at least one selectron or sneutrino whose masses are large of the order of the supersymmetry breaking scale. Our previous considerations on the TGV's has shown that sleptons yield smaller contributions as compared to other sectors and especially that of the neutralinos and charginos. On these grounds we expect a small effect from the supersymmetric box graphs in which sleptons are exchanged. Indeed it has been shown[26] that the effect of some supersymmetric boxes is quite small at LEP200 energies. At NLC energies however these become comparable to the TGV contributions. Therefore for a complete phenomenological study their contributions should be taken into account. The effect of the box graphs on the TGV form factors entering into $e^+e^- \rightarrow W^+W^-$ is under study and the results will appear in a future publication.

Our conclusion concerning the trilinear gauge boson vertices is that for energies $2M_W < \sqrt{s} < 200\ GeV$ the MSSM predictions differ in general from those of the SM but they are of the same order of magnitude. To be detectable deviations from the SM requires sensitivities reaching the per mille level and hence unlikely to be observed at LEP200. If deviations from the SM predictions are observed at these energies it will be a signal of new underlying dynamics, which however will not be of supersymmetric nature. At higher energies SM and MSSM predictions fall rapidly to zero, due to unitarity, getting smaller, in most cases, by almost an order of magnitude already at energies $\sqrt{s} \approx 0.5\ TeV$. As a result, the task of observing deviations from the SM which are due to supersymmetry demands higher experimental accuracies as well as a complete theoretical treatment which properly takes care of box contributions.

Acknowledgements

References

[1] W. Hollik, in *"Lepton and Photon Interactions"*, Proceedings of the XVI International Symposium, Ithaca, New York, 1993, ed. by P. Drell and D. Rubin, AIP Conf. Proc. No. 302 (AIP, New York, 1994);
D. Scaile, in *Proceedings of the International Symposium on Vector Boson self Interactions*, UCLA, Los Angeles, February 1-3 1995 (to appear).

[2] M. Schwarz, in *"Lepton and Photon Interactions"* [1].

[3] M. Davier and D. Treille, in *Proceedings of the ECFA workshop on LEP200*, Aachen, Germany 1986, ed. by A. Böhm and W. Hoogland (CERN Report No 87-08, Geneva, Switzerland).

[4] M. Bilenky, J. L. Kneur, F. M. Renard and D. Schildknecht, Nucl. Phys. B409 (1993) 22; BI-TP 93/43, PM 93/14 (preprint); G. L. Kane, J. Vidal and C. P. Yuan, Phys. Rev. D39 (1989) 2617; J. Busenitz, in *Proceedings of the International Symposium on Vector Boson self Interactions* [1].

[5] J. Fleitcher, J. L. Kneur, K. Kolodziej, M. Kuroda and D. Schildknecht, Nucl. Phys. B378 (1992) 443; D. Zeppenfeld, in *Proceedings of the International Symposium on Vector Boson self Interactions* [1]; S. Godfrey, *ibid.* ; J. Womersky, *ibid.* ; T. Barklow, *ibid.*

[6] UA2 collaboration, Phys. Lett. B227 (1992) 191;
CDF and D0 collaborations, S. Errede in *Proceedings of the 27th International Conference on High Energy Physics*, Glasgow, Scotland, July 20-27, 1994.

[7] K. F. Gaemers and G. J. Gounaris, Z. Phys. C1 (1979) 259; K. Hagiwara, R. D. Peccei, D. Zeppenfeld and K. Hikasa, Nucl. Phys. B282 (1987) 253; U. Baur and D. Zeppenfeld, Nucl. Phys. B308 (1988) 127; B325 (1989) 253; D. Zeppenfeld, Phys. Lett. B183 (1987) 380.

[8] D. Zeppenfeld and S. Willenbrock, Phys. Rev. D37 (1988) 1775; A. F. Falk, M. Luke and E. H. Simmons, Nucl. Phys. B365 (1991) 523; E. N. Argyres and C. G. Papadopoulos, Phys. Lett. B263 (1991) 298; A. de Rujula, M. B. Gavela, P. Hernandez and E. Masso, Nucl. Phys. B384 (1992) 298; G. Gounaris and F. M. Renard, Z. Phys. C59 (1993) 143; G. Gounaris, J. Layssac and F. M. Renard, Univ. of Monpellier PM 93/26, (preprint).

[9] For reviews see:
H. P. Nilles, Phys. Rep. 110 (1984) 1 ; H. E. Haber and G. L. Kane, Phys. Rep. 117 (1985) 75 ; A. B. Lahanas and D. V. Nanopoulos, Phys. Rep. 145 (1987) 1.

[10] J. Ellis, S. Kelley and D. V. Nanopoulos, Phys. Lett. B260 (1991) 131; U. Amaldi, W. De Boer and M. Fürstenau, Phys. Lett. B260 (1991) 447; P. Langacker and M. Luo, Phys. Rev. D44 (1991) 817.

[11] E. N. Argyres, G. Katsilieris, A. B. Lahanas, C. G. Papadopoulos and V. C. Spanos, Nucl. Phys. B391 (1993) 23.

[12] A. B. Lahanas and V. C. Spanos, Phys. Lett. B334 (1994) 378; A. B. Lahanas, in *Proceedings of the International Symposium on Vector Boson self Interactions* [1], and references therein.

[13] W. A. Bardeen, R. Gastmans and B. Lautrup, Nucl. Phys. B46 (1972) 319.

[14] G. Couture and J. N. Ng, Z. Phys. C35 (1987) 65.

[15] A. Culatti, Padova University preprint, DFPD/94/TH/25.

[16] J. M. Cornwall, in *Deeper Pathways in High Energy Physics* edited by B. Kursunoglou, A. Perlmutter and L. Scott (Plenum, N.Y. 1977), p. 583; Phys. Rev. D26 (1982) 1453; J. M. Cornwall, W. S. Hou and J. E. King, Phys. Lett. B153 (1988) 173; J. M. Cornwall and J. Papavassiliou, Phys. Rev. D40 (1989) 3474.

[17] J. Papavassiliou and K. Philippides, Phys. Rev. D48 (1993) 4255; N.Y. University preprint hep-ph/9503246; J. Papavassiliou, Phys. Rev. D50 (1994) 5958; J. Papavassiliou, in *Proceedings of the International Symposium on Vector Boson self Interactions* [1]; K. Philippides, *ibid.*

[18] G. Degrassi and A. Sirlin, Phys. Rev. D46 (1992) 3104. J. Papavassiliou and C. Parrinelo, Phys. Rev. D50 (1994) 3059; G. Degrassi, B. Kniehl and A. Sirlin, Phys. Rev. D48 (1993) R3963; J. Papavassiliou and A. Sirlin, Phys. Rev. D50 (1994) 5951.

[19] N. J. Watson, Phys. Lett. B349 (1995) 155.

[20] A. Drenner, G. Weiglein and S. Dittmaier, Phys. Lett. B333 (1994) 420; BI-TP.94/50, UWITP 94/03 hep-ph/9410338;
S. Hashimoto, J. Kodaira, Y. Yasui and K. Sasaki, Phys. Rev. D50 (1994) 7066.

[21] F. Abe et. al, CDF collaboration, Phys. Rev. Lett. 74 (1995) 2626;
S. Abachi et. al, D0 collaboration, Phys. Rev. Lett. 74 (1995) 2632.

[22] G.Gounaris et *al.*, 'Triple Gauge Boson Couplings', hep-ph/9601233, to appear in "Physics at LEP2", G. Altarelli and F. Zwirner eds., CERN Report 1996

[23] H. Aihara et al., FERMILAB-Pub-95/031, MAD/PH/871, UB-HET-95-01, UdeM-GPP-TH-95-14, 1995.

[24] M. Lemoine and M. Veltman, Nucl. Phys. B164 (1980) 445;
M. Böhm, A. Denner, T. Sack, W. Beenakker, F. Berends and H. Kuijf, Nucl. Phys. B304 (1988) 463.

[25] J. Fleitcher, F. Jegerlehner and M. Zralek, Z. Phyzik C42 (1989) 409;
J. Fleitcher, K. Kolodziej and F. Jegerlehner, Phys. Rev. D47 (1993) 830;
ibid. D49 (1994) 2174.

[26] A. Ahrib,J.-L. Kneur and G. Multaka, CERN-TH/95-344, to appear in Physics Letters B.

$A_0, m_0, M_{1/2}$	$\tan\beta = 2\ m_t = 170\,GeV$					
	300, 300, 80		300, 300, 300		0,0,300	
	$\mu > 0$	$\mu < 0$	$\mu > 0$	$\mu < 0$	$\mu > 0$	$\mu < 0$
	$\sqrt{s} =190$GeV					
Δk_γ	-1.989	-1.783	-1.793	-1.818	-1.812	-1.841
ΔQ_γ	0.903	0.297	0.523	0.525	0.534	0.537
Δk_Z	-2.359	-2.065	2.209	-2.196	-2.208	-2.189
ΔQ_Z	-0.366	-1.197	0.342	0.360	0.331	0.354
SM predictions	$\Delta k_\gamma = -2.005, -1.735, -2.118\ \ \Delta Q_\gamma = 0.524, 0.530, 0.503$					
	$\Delta k_Z = -1.350, -2.437, -1.404\ \ \Delta Q_Z = 0.507, 0.533, 0.481$					
	$\sqrt{s} =500$GeV					
Δk_γ	-0.262	-0.310	-0.151	-0.207	-0.191	-0.259
ΔQ_γ	0.150	0.146	0.030	0.041	0.056	0.069
Δk_Z	0.115	0.238	0.198	0.191	0.203	0.198
ΔQ_Z	0.362	0.256	-0.407	-0.325	-0.427	-0.352
SM predictions	$\Delta k_\gamma = -0.250, -0.168, 0.046\ \ \ \Delta Q_\gamma = 0.054, 0.057, 0.064$					
	$\Delta k_Z = 0.147, 0.208, -0.036\ \ \ \Delta Q_Z = 0.057, 0.058, 0.077$					

Table 1: MSSM predictions for $\Delta k_{\gamma,Z}$, $\Delta Q_{\gamma,Z}$, in units of $g^2/16\pi^2$, for three different inputs of $A_0, m_0, M_{1/2}$ (in GeV), at LEP2 and NLC energies. Both $\mu > 0$ and $\mu < 0$ cases are displayed. The SM predictions for Higgs masses $50, 100$ and $300\ GeV$ respectively are also displayed.

Figure Captions

Figure 1: The kinematics of the WWV vertex. $P_{1,2,3}$ denote internal particle lines.

Figure 2: **a)** MSSM predictions for the real part of Δk_γ (solid lines) and Δk_Z, (dashed lines), in units of $g^2/16\pi^2$, as functions of the energy $\sqrt{s}$. The inputs are $(A_0, m_0, M_{1/2}) = (300, 300, 80)\ GeV$, $\tan\beta = 2$, $m_t = 170\,GeV$. Only the MSSM case $\mu > 0$ is displayed. The vertical dotted line indicates the position of the WW production threshold. **b)** SM predictions for $m_t = 170$GeV and SM Higgs mass, $m_H = 100$GeV.

Figure 3: $\Delta k_\gamma - 4Q^2/(4Q^2 - m_Z^2)\Delta k_Z$ as a function of the energy, for the SM (solid line), MSSM with $\mu > 0$ (dashed line) and MSSM with $\mu < 0$ (dashed doted line). The MSSM parameters are as in Figure 2. The standard model Higgs mass is taken $100GeV$.
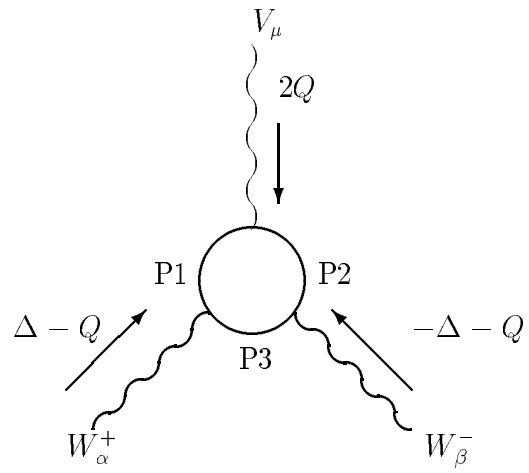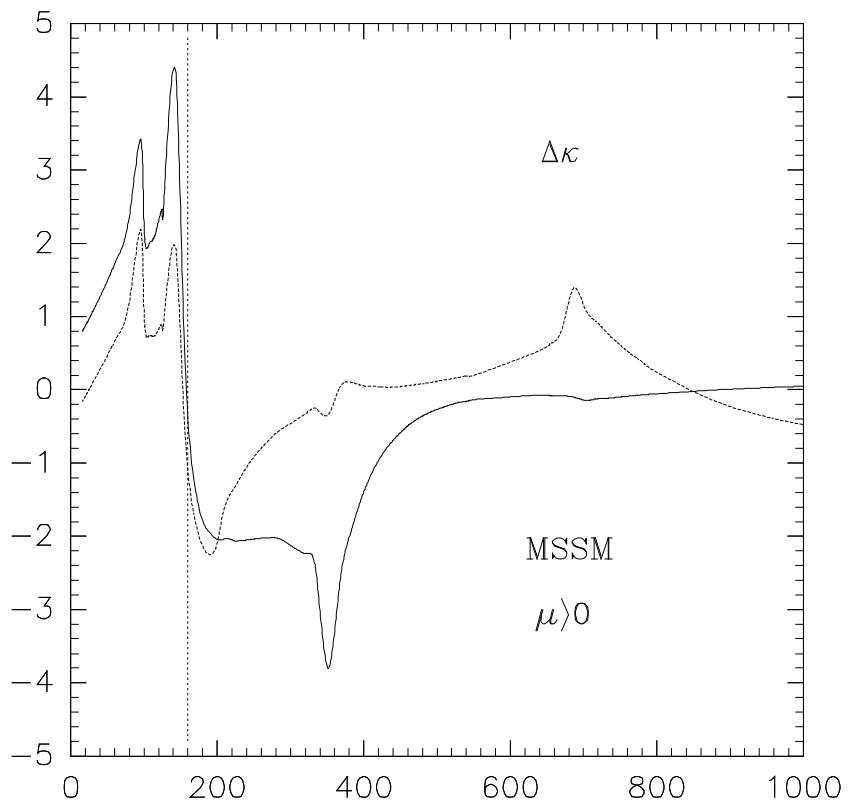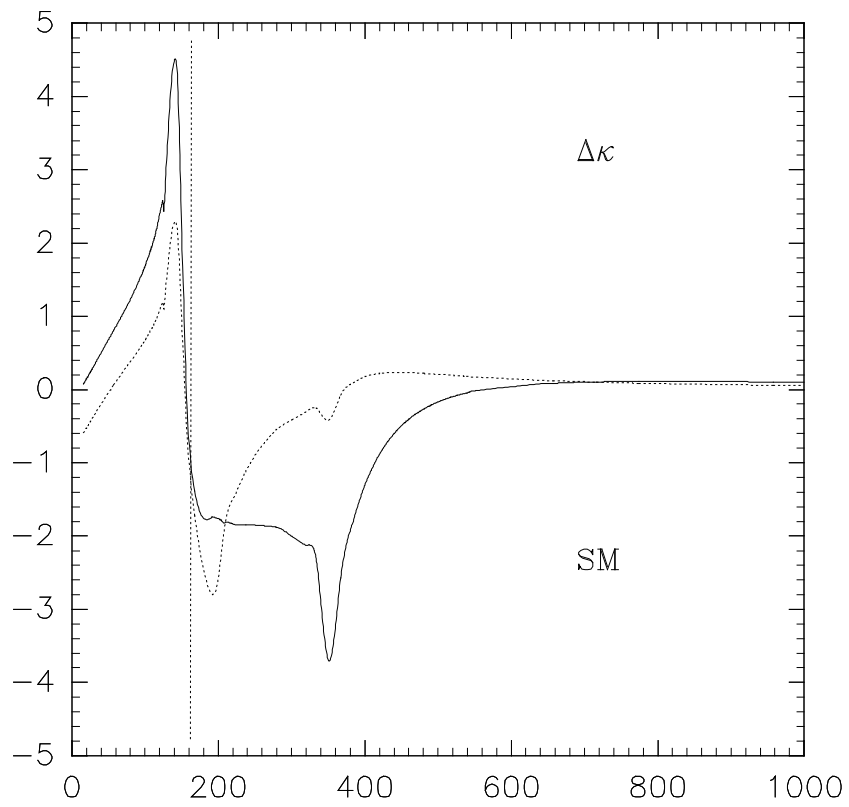
V_μ

$2Q$

P1 P2

$\Delta - Q$ $-\Delta - Q$

P3

W_α^+ W_β^-

Figure 1

(a)

(b)

Figure 2

SM

MSSM ($\mu\rangle0$)

MSSM ($\mu\langle0$)

Figure 3